ELSEVIER

Signal Processing 82 (2002) 1317–1328

SIGNAL PROCESSING

www.elsevier.com/locate/sigpro

Generalization of Canny–Deriche filter for detection of noisy exponential edge

E. Bourennane*, P. Gouton, M. Paindavoine, F. Truchetet

Université de Bourgogne Laboratoire LE2I, Fac. des Sciences et Techniques, BP 47870, 21078 Dijon Cedex, France

Received 9 July 1997; received in revised form 4 September 2000

Abstract

This paper presents a generalization of the Canny–Deriche filter for ramp edge detection with optimization criteria used by Canny (signal-to-noise ratio, localization, and suppression of false responses). Using techniques similar to those developed by Deriche, we derive a filter which maximizes the product of the first two criteria under the constraint of the last one. The result is an infinite length impulse response filter which leads to a stable third-order recursive implementation. Its performance shows an increase of the signal-to-noise ratio in the case of blurred and noisy images, compared to the results obtained from Deriche's filter.

1. Introduction

Among the image processing stages involved in an artificial vision system, edge detection is one of the most useful and basic. The edges or contours are characterized by sharp and wide variations of luminance in the image. The detection and localization of these variations in luminance have been the subjects of numerous publications. Gradient estimations (Roberts' gradient for instance [13]) are the classical methods which give satisfactory results in the case of slightly noisy images. In the case of heavily noised images, researchers have developed different optimal operators by associating low-pass filtering with the gradient detector [10,15,8]. Briefly we will review some recent developments in this field.

In 1986, Shen and Castan [16] proposed a filter with exponential impulse response in order to detect step edges using a second derivative filter. In order to implement this filter, they proposed a design based on a recursive form (a first-order filter). The results obtained showed a good resistance to noise and a good localization of contours, but the optimality was not clearly defined.

Canny [3] was the first to give analytic expressions for the criteria that have to be optimized in edge detection. He defined three criteria: signal-to-noise ratio (SNR) after detection, localization (L) of the detected edge with respect to the theoretical one, and mean distance between multiple responses of the detector and the real edge multiple response criterion (MRC) [3].

The application of these three criteria to an ideal edge (step edge) has led to the development of an optimal filter defined by its finite impulse response.

An unlimited band (from the spatial point of view) extension of Canny's filter was proposed by Deriche in 1987 [5,6]. In order to avoid truncating the filter, Deriche used a second-order recursive implementation. The results obtained showed a great improvement compared to those obtained by Canny, particularly for the reduction of multiple responses.

* Corresponding author. Tel./fax: +03-80-39-60-04.
E-mail address: ebourenn@u-bourgogne.fr (E. Bourennane).

0165-1684/02/$ - see front matter
PII: S0165-1684(02)00283-9

The authors quoted above based their studies on the detection of ideal edges which are hardly consistent with those encountered in real images. This led Petrou and Kittler [11] to propose in 1991 a more general optimum filter for smooth edges. Their optimization is oriented by using the criteria defined by Canny. The result is given in the form of a table of convolution masks based on the truncation of the filter impulse response. The results presented are thus largely incomplete with respect to obtaining different slopes of a particular edge. Furthermore, it appears that the comparison of their filter with that of Deriche's is based on a bad choice of parameters for the latter.

We propose to resume again the study described above by using the same edge model. This edge model depends on a parameter s, which describes the blur (the shape of the edge) in the image. This blur may result from the real shape of the objects or from their movement during the shot; it can also be due to the lens's limited field depth, or to the fact that the camera is out of focus. A non-punctual light source is also a common source of blurred object contours.

We believe that the method used by Petrou and Kittler [11] is not the best. We propose here a third-order recursive filter which improves, in terms of sensitivity, the detection (in the sense of Canny's criteria) with respect to a Deriche filter (optimized correctly for the chosen edge) and with Petrou and Kittler's filter.

2. Optimization criteria of the edge detector

2.1. Real edge

The acquisition of a real world image by an optical system implies the presence of a certain blur, generally modeled by: $J_1(x)/x$ (where J represents a Bessel function). Here, we use a Gaussian filter as an approximation of the optical blurring. However, as noted previously, the blur in real edges can have other causes than optical ones. This is why this model can only represent aspect of real cases in an approximate way, and any other model which approximates reality in the same way can be used.

Essentially, for the simplification of calculations, we have chosen the following edge function [17]:

$$C(x) = \begin{cases} 1 - \dfrac{e^{-sx}}{2} & \text{for } x \geqslant 0, \\ & \text{with } s > 0, \\ \dfrac{e^{sx}}{2} & \text{for } x < 0. \end{cases} \tag{1}$$

In Fig. 1, we show the influence of the parameter s on the edge model (the line curve is obtained for $s = 0.5$ and the point curve for $s = 5$).

The choice of our model is illustrated by the ball (picture) shown in Fig. 2 associated with the profile

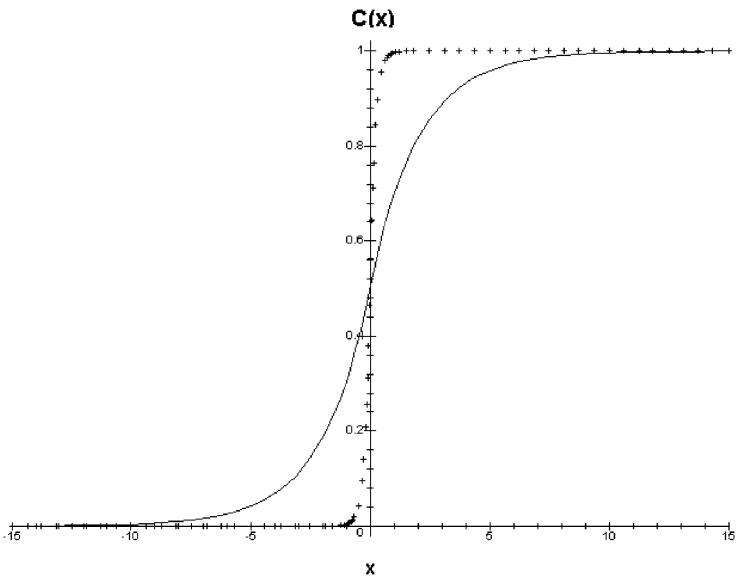

Fig. 1. The edge model function (line curve $s = 0.5$ point curve $s = 5$).

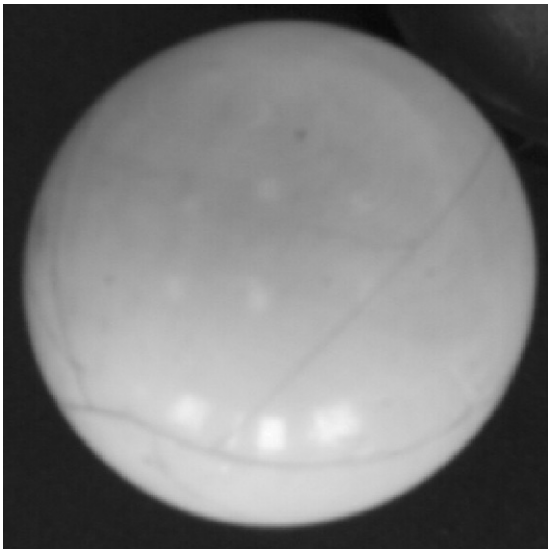

Fig. 2. Real image, which represents an image ball captured with a CCD camera.

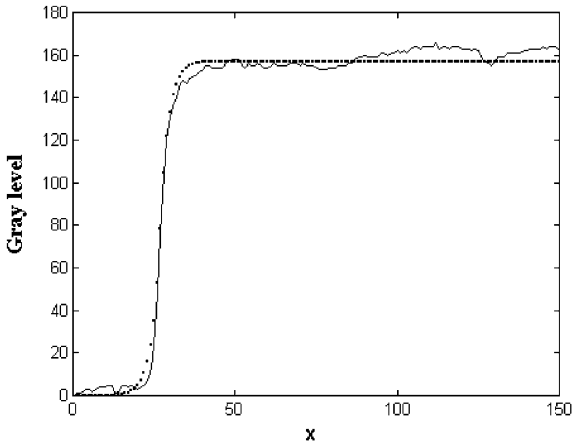

Fig. 3. A cross-section of the ball image shows its edge profile (line curve: cross-section point curve: exponential edge model for $s = 0.4$).

given in Fig. 3 (the line curve is the real profile, and the point curve is the exponential edge function obtained with $s = 0.4$).

2.2. Optimization criteria

We are looking for a real one-dimensional linear filter with which to start. Since we are interested in the local maxima at the output of this filter, it must satisfy the following conditions [19]:

Its impulse response $f(x)$ must be odd:

- $f(x) = -f(-x)$ then $f(0) = 0$.
- Its impulse response must vanish at $\pm\infty$, and preferably it must have only a single zero.
- The maximum response to a step edge must be unique: $f(0) = 0$, $f'(0) = 0$, and $f'(\infty) = 0$.

These optimization criteria are the same as those given by Canny [3] and by Petrou and Kittler [11].

2.2.1. For SNR

The input signal is the edge defined in Eq. (1). The noise is assumed to be additive, Gaussian, and zero mean (this hypothesis is correct for usual noisy images, but it is evidently false in the case of textured images).

The SNR at $x = 0$ is therefore given by (2):

$$\mathrm{SNR} = \frac{|\int_{-\infty}^{+\infty} C(-x) f(x)\,\mathrm{d}x|}{n_0(\int_{-\infty}^{+\infty} f^2(x)\,\mathrm{d}x)^{1/2}} = K_1 \Sigma, \tag{2}$$

where n_0^2 is the power spectrum density of the additive white noise, $K_1 = 1/\sqrt{2}n_0$, and Σ is the variable part which must be maximized during the optimization process.

2.2.2. For localization

This criterion must characterize the average difference between the position of the detected edge in the presence of noise and its exact position. In order to have an expression to be maximized, Canny [3] considered the localization as being the inverse of the variance of the detected edge position. The parameter L defined by Eq. (3) must be as large as possible:

$$L' = \frac{|\int_{-\infty}^{+\infty} C'(-x) f'(x)\,\mathrm{d}x|}{n_0(\int_{-\infty}^{+\infty} f'^2(x)\,\mathrm{d}x)^{1/2}} = K_1 L. \tag{3}$$

2.2.3. For the multiple response criterion

In the presence of noise, the detected signal can show several maxima. These false responses must be as distant as possible from the main one. The MRC, defined by expression (4), is proportional to the average distance between maxima of the filter's response to Gaussian white noise. For $x < 0$, the MRC must

therefore be maximized [3,5]

$$\mathrm{MRC} = \left(\frac{|\int_{-\infty}^{0} |f'^2(x)\,\mathrm{d}x|}{\int_{-\infty}^{0} f''^2(x)\,\mathrm{d}x} \right)^{1/2}. \tag{4}$$

The optimum filter is obtained by maximizing each of these three criteria equations (2)–(4). For calculation simplification reasons, Canny proposed the maximization of the product $\Sigma \cdot L$ under the MRC constraint which is effected to an arbitrary constant.

Note that in 1990 Tagare and De Figueiredo [18] proposed a modification of Canny's localization criterion. Their criterion is based on a statistical study of the number of zero crossings of the first derivative of the filter's response to noisy input. The form of the criterion which they proposed concerned only ideal edges, and their method was thus not general. On the other hand, Sarkar and Boyer in 1991 [14] proposed a modification of the MRC by introducing the notion of an equivalent band (in the spatial domain). Using variational calculus, they designed a filter (a table of values representing the parameters of the filter) which is difficult to implement. So they proposed (without any theoretical justification) a recursive implementation of a third-order filter.

The MRC criterion proposed by Sarkar and Boyer is not in agreement with that proposed by Canny. To see that, it suffices to look at Figs. 3 and 4 [14, p. 1160] and notice that their MRC increases when the filter becomes narrow in the spatial domain! The MRC would logically have to decrease because the filter becomes more and more high-pass (in frequency); as a result, it passes more noise and reduces the maximal average distance (therefore the MRC) that separates two adjacent zero crossings. Sarkar and Boyer's MRC evolves in a contradictory manner as compared to the evolution of Canny 's.

In the Rice (Canny) [12] proposal, the wider the band of the filter, the more the distance $x_{\max}(f)$ decreases as opposed to what occurs in the Sarkar and Boyer's criterion.

3. Filter impulse response

The optimization concerns only the variable parts of the three criteria. We choose to maximize the product $\Sigma \cdot L$ under the MRC constraint. Thus, we transform the optimization problem into a problem under constraints which use variational calculus [4] requiring the calculation of a functional in the admissible functions domain. Thus, one of the integrals of the expression $\Sigma \cdot L$ should be optimized while leaving the others as undetermined constants. Finally, we choose to minimize one of the denominator integrals of the $\Sigma \cdot L$ with the constraints C1–C4 (for $x \leqslant 0$):

$$\int_{-\infty}^{0} f^2(x)\,\mathrm{d}x$$

$$C_1 = \int_{-\infty}^{0} f(x)(1 - \mathrm{e}^{sx})\,\mathrm{d}x, \quad C_2 = \int_{-\infty}^{0} f(x)\mathrm{e}^{sx}\,\mathrm{d}x,$$

$$C_3 = \int_{-\infty}^{0} f''^2(x)\,\mathrm{d}x, \quad C_4 = \int_{-\infty}^{0} f'^2(x)\,\mathrm{d}x. \tag{5}$$

The C_i $(i = 1,\ldots,4)$ are arbitrary constants. By using Lagrange multipliers [4], the composite function is formed (6):

$$Z(x, f, f', f'') = f^2(x) + \lambda_1 f'^2(x) + \lambda_2 f''^2(x) + \lambda_3 f(x)\mathrm{e}^{sx} + \lambda_4 f(x)(1 - \mathrm{e}^{sx}). \tag{6}$$

This function must satisfy the Euler equation (given in Appendix A) which leads to a differential equation with $f(x)$ as a solution. The general form obtained for $f(x)$ is given here (the details of the calculations are given in Appendix A):

$$2f - 2\lambda_1 f'' + 2\lambda_2 f'''' = (\lambda_4 - \lambda_3)\mathrm{e}^{sx} - \lambda_4. \tag{7}$$

To solve this differential equation, one seeks conditions of existence of the general equation without second member:

$$2f - 2\lambda_1 f'' + 2\lambda_2 f'''' = 0$$

f is replaced by a particular solution, which leads to the next characteristic equation:

$$1 - \lambda_1 \xi^2 + \lambda_2 \xi^4 = 0 \quad \text{with } \xi = \pm\alpha \pm \mathrm{i}\omega. \tag{8}$$

This leads to expressions of λ_1 and λ_2

$$\lambda_1 = \frac{2(\alpha^2 - \omega^2)}{4\alpha^2\omega^2 + 4(\alpha^2 - \omega^2)^2}, \qquad \lambda_2 = \frac{1}{4\alpha^2\omega^2 + 4(\alpha^2 - \omega^2)^2}. \tag{9}$$

The final solution leads to the function $f(x)$ hereafter. By taking into account the boundary conditions, the number of constants is reduced:

$$f(x) = a_1 e^{\alpha x}\sin(\omega x) + a_2 e^{\alpha x}\cos(\omega x) - a_2 e^{sx} \quad \text{with } x \leqslant 0 \text{ and } a_i = \text{constant}, \tag{10}$$

$$a_2 = \frac{\frac{1}{3}\lambda_3}{1 + s^2(s^2\lambda_2 - \lambda_1)}. \tag{11}$$

4. Parameters estimation and limit conditions

The search for the best filter leads to the determination of the parameter values which maximize the three initial criteria. According to Canny [3], this consists of maximizing the product $\Sigma \cdot L$ under the MRC constraint. For this, we replace the function $f(x)$ by its value and calculate the product $\Sigma \cdot L$. Then, we would like to analyze the different functions obtained, starting with the three optimization criteria. Prior to all these steps, we simplify the problem by limiting the variation range and by setting the limit conditions.

Eqs. (9) and (11) allowed us to decrease the number of parameters on which f depends; f does not depend on more than five parameters (a_1, ω, α, s and λ_3). Still, optimal solution of f seems difficult to reach because it depends on five variables. In order to find the function f, we are going to proceed to other simplifications.

First of all, this filter is conceived to analyze images. The standard system of acquisition provides images whose sizes vary between 512 and 1024 pixels. In numerical approaches, the pixel represents the unit of length. One of the conditions for good filter effectiveness is a unique maximum for step response, which is equivalent to the condition of unique zero crossing in the impulse response (for finite x). This zero crossing must correspond to $x = 0$. If we take into account the image size, ω must be very small ($\omega < 1/1024$) in order to respect the above condition.

By taking into account the previous consideration, and for finite x, we deduce that $\omega x \ll 1$, which leads to the next solution of f:

$$f(x) = a_1 e^{\alpha x}\omega x + a_2 e^{\alpha x} - a_2 e^{sx} \quad \text{for } x \leqslant 0, \tag{12}$$

where $\sin(\omega x) \cong \omega x$ and $\cos(\omega x) \cong 1$.

The value a_1 is a non-null constant, and a new function defined by $f/\omega a_1$ is also an optimal function in the senses of the three criteria. All these hypotheses lead to this final function:

$$f(x) = (x + A)e^{\alpha x} - Ae^{sx}. \tag{13}$$

As $\omega \ll 1$ in order to avoid oscillations then

$$\lambda_1 \approx \frac{1}{2\alpha^2}, \quad \lambda_2 \approx \frac{1}{4\alpha^4},$$

with

$$A = \frac{4}{3}\frac{k\alpha^4}{\omega(4\alpha^4 + s^4 - 2s^2\alpha^2)}, \qquad k = \frac{\lambda_3}{a_1}.$$

For an ideal edge with a parameter s equal to infinity, the function is equivalent to

$$f(x) = xe^{\alpha x}. \tag{14}$$

This function is also the first-order approximation of the Deriche filter [6].

5. Numerical approach to the influence of parameters α and k on optimization criteria

After simplification f depend only on three variables: α, k, and s. In order to take into account the previous remark, the value 10^{-4} is arbitrarily chosen for ω in the following sections.

Parameter s is a characteristic of each given image, and in certain cases it is even object dependent. Indeed, as noted above, the reasons for edge blurring can be multiple: optical, linked to the shape of the objects being viewed, related to the same movements, or even due to illumination characteristic.

Therefore the choice of the value for s has been made either in an "ad hoc" manner or in accordance with some modelization of the scene. Some trivial experiments have been done in order to avoid this "a priori" and the multi-resolution approach seems to be interesting [20,7].

In this paper, which is concerned with optimal edge detection, we assume that s is known and we try to study how to chose α and k for optimal edge detection.

Given the complex form of the product $\Sigma \cdot L$, it is impossible to obtain an analytic solution. So we use here a numerical approach to solve this problem. For

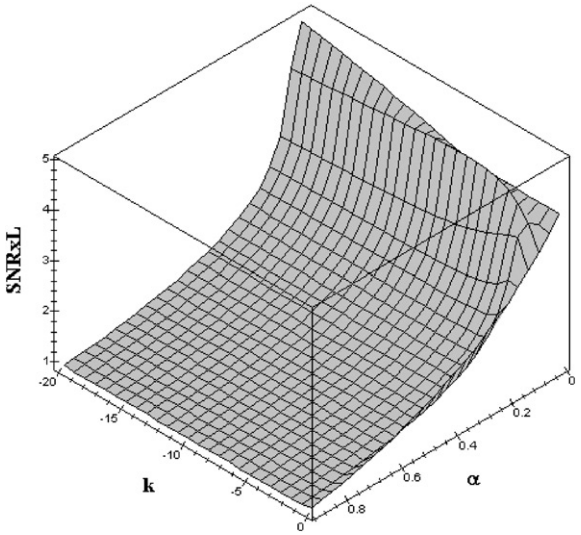

Fig. 4. Effect of k and α on the product SNR by L.

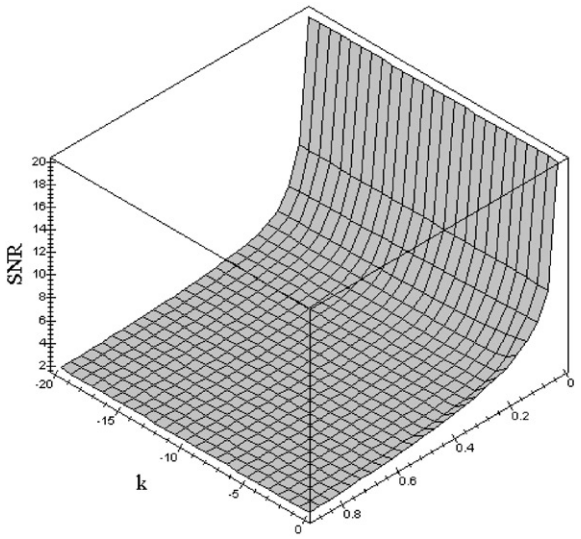

Fig. 5. Effect of k and α on the SNR.

several values of $s = 1$, we give a numerical representation of $\Sigma \cdot L$ in Fig. 4. The first analysis shows that the product increases with decreasing α and increasing k. The better we know this characteristic, the easier it is to detect the edges in the images. Figs. 5 and 6 show the effect of α and k on SNR and L (localization).

In Figs. 5 and 6 we observe that the localization criterion (L) decreases with decreasing α. At the same

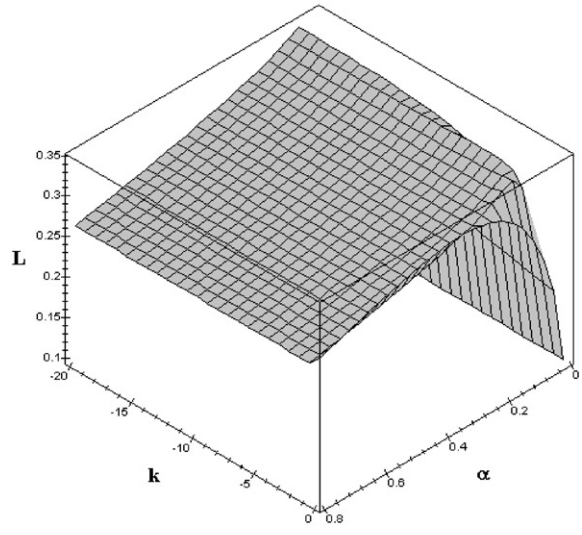

Fig. 6. Effect of k and α on (L).

time, we observe the opposite phenomenon according to the SNR criterion, so the best choice of α depends on the type of image.

The best advantage of this filter resides in the fact that it takes into account the effect of the physical defects of the blurred images before detecting the edges. In this way, we separate the trade-off problems of the SNR and localization.

We can illustrate the effect of the parameter s introduced here in our filter function with the choice of two different values. For example, a blurred image is characterized by: $s = 1$, $\alpha = 0.06$, and $k = -20$; the product of the SNR by the localization is equal to 5.26. Consequently, for an ideal edge model (Deriche's approach), applied to detect a blurred image is equal to 3.56, corresponding to a decrease of 32%. For common images, the s is finite, so using our edge model leads to increasing the SNR criterion which is predominant compared to the localization one.

Fig. 7 represents the product $\Sigma \cdot L$ for a fixed $k = -20$. The curve in full line is obtained with the function filters developed. The dotted line corresponds to the Deriche filter. Compared to the Deriche filter whose $\Sigma \cdot L$ is limited to 4, the general filter one obtains a better product.

Fig. 8 deals with the optimal function with real $s = 0.5$, $\alpha = 0.15$, and $k = -1$ (continuous line), and its approximation to ideal edge (dotted line).

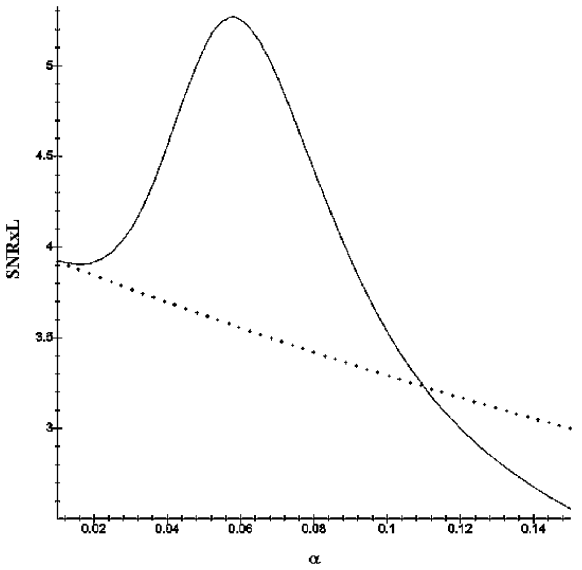

Fig. 7. Influence of a on the product RSB $\times L$ for a fixed $k=-10$ (line curve general filter, point curve represents Deriche' ones).

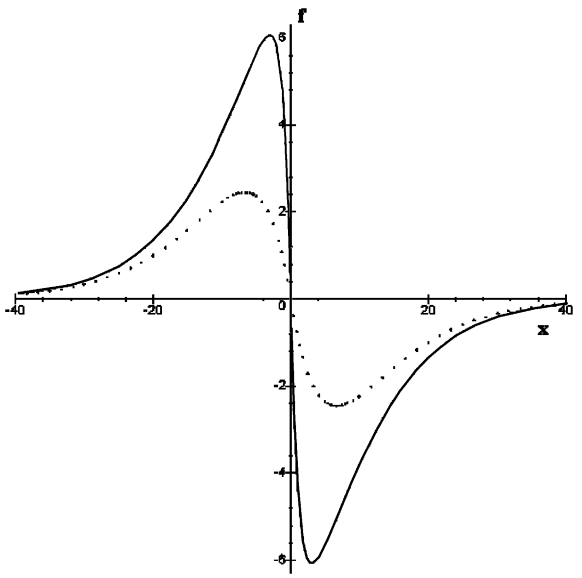

Fig. 8. The filter function (line curve general filter with $s=1$ and $k=-1$, point curve represents Deriche' ones $k=0$).

6. Implementation in recursive form

Given the filter function $f(x)$ obtained by Eq. (13), an infinite impulse response (IIR) filter is obtained by sampling $f(x)$ (see Fig. 8) with a unity sampling period. Its impulse response is given by $f(n)$ with n being an integer.

The normalization can be effected by multiplying by a constant G (see Appendix B), such that

$$\sum_{-\infty}^{+\infty} Gf(n)C(-n)=1. \tag{15}$$

Taking the z transform (TZ) of $f(n)$ split in causal and anti-causal part yields

$$f^-(n)=-(n+A)\mathrm{e}^{\alpha n}+A\mathrm{e}^{sn} \quad \text{with } n\leqslant 0, \tag{16}$$

$$f^+(n)=(-n+A)\mathrm{e}^{-\alpha n}-A\mathrm{e}^{-sn} \quad \text{with } n>0. \tag{17}$$

Only the TZ of the causal part is calculated; that of the anti-causal part is deduced

$$\begin{aligned}
&\mathrm{TZ}(f^+)=\sum_{-\infty}^{+\infty} f^+(n)z^{-n}=\mathrm{TZ}^+,\\
&\mathrm{TZ}(f^-)=\mathrm{TZ}^-=-\mathrm{TZ}^+\left(\frac{1}{z}\right),\\
&\mathrm{TZ}^+=\frac{a_1z^{-1}+a_2z^{-2}}{1-a_3z^{-1}+a_4z^{-2}-a_5z^{-3}}=\frac{Y^+(z)}{X(z)},\\
&\mathrm{TZ}^-=-\frac{a_1z+a_2z^2}{1-a_3z+a_4z^2-a_5z^3}=\frac{Y^-(z)}{X(z)},
\end{aligned} \tag{18}$$

where $X(z)=\mathrm{TZ}(x)$ and $Y(z)=\mathrm{TZ}(y)$; x and y being the input and the output signals of the filter ($Y(z)=Y^+(z)+Y^-(z)$).

Finally, the following stable third-order recursive filter is obtained:

$$\begin{aligned}
y^+(i)&=a_1x(i-1)+a_2x(i-2)-a_3y^+(i-1)\\
&\quad -a_4y^+(i-2)-a_5y^+(i-3),\\
y^-(i)&=a_1x(i+1)-a_2x(i+2)-a_3y^-(i+1)\\
&\quad -a_4y^-(i+2)-a_5y^-(i+3),
\end{aligned} \tag{19}$$

where a_i are given in Appendix B.

7. 2-D Extension

The one-dimensional filter $f(x)$, presented in Section 3, allows us to obtain the directional derivative in

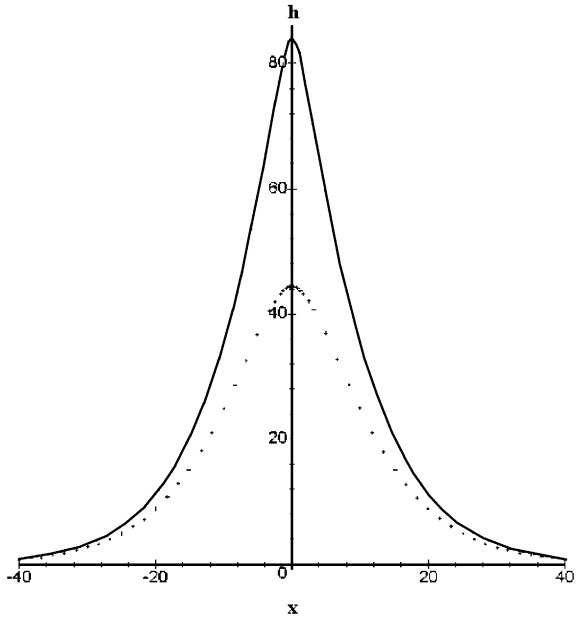

Fig. 9. The smoothing function (line curve general filter with $s=1$ and $k=-1$, point curve represents Deriche' ones $k=0$).

the x-axis direction. Each point on an edge within a 2-D image is defined by its gray level, its position, and the orientation of the gradient in its neighborhood. Because all orientations are possible within the image, it is preferable for the operator to be symmetrical (circularity symmetric) in all directions. Torre and Poggio [19] showed the necessity of using a regularizing filter before taking a derivative (see also [9]). Knowing that it is difficult to extend isotropically an odd filter to 2-D (whereas an even filter can be extended by a simple rotation), we prefer to find an even regularization filter starting with our odd filter $f(x)$. For this, we use the convolution property

$$f(x) * I(x) = \frac{\mathrm{d}(h(x) * I(x))}{\mathrm{d}x} = \frac{\mathrm{d}h(x)}{\mathrm{d}x} * I(x)$$

with

$$\frac{\mathrm{d}h(x)}{\mathrm{d}x} = f(x) \text{ and } I(x) \text{the image.}$$

Calculating the integral of the above expression, one can obtain the following regularization filter (Fig. 9):

$$h(x) = -\frac{(s\alpha x - s + s\alpha A)\mathrm{e}^{\alpha x} - (A\alpha^2)\mathrm{e}^{sx}}{s\alpha^2}. \qquad (20)$$

The recursive implementation of the regularization filter leads to the same causal/anti-causal decomposition.

We want to maintain the separability of our function for simplicity and calculation load. Therefore, knowing that the direction of an edge as well as the amplitude of the gradient can be calculated in two arbitrary perpendicular directions, the derivative along column (c) is determined by a smoothing operation along row (r) and vice versa. From the separability of the function, the smoothing function in 2-D is deduced from:

$$L(m,n) = h(m) \cdot h(n).$$

The derivative in c and r directions gives the following 2-D, separable filters:

$$L_c(m,n) = f(m) \cdot h(n),$$

$$L_r(m,n) = h(m) \cdot f(n)$$

m and n being the index for column and row, respectively.

8. Experiments and results

All images processed here are gray level images with a 256 gray scale and in a 256×256 pixels format. Fig. 10 represents a real world image (French research group GDR ISIS) with an additive Gaussian noise of standard deviation $\sigma = 50$. This additive noise has been created with a white-noise Gaussian generator, and this noise is independent of the original image.

Fig. 11 represents the edges detected using the ideal camera with $s \to \infty$ and $\alpha = 0.1$ and $k = -1$, by the filter $f(x)$ (which corresponds to Deriche's filter), whereas Fig. 12 represents those obtained using a real camera with $s = 0.5$. Note that Fig. 12 is less noisy than Fig. 11.

The second result represents a ball picture which has been chosen for the illustration of the blurred scene (Fig. 2). This image has been disturbed by an additive Gaussian noise of standard deviation $\sigma = 50$ (Fig. 13). Figs. 14 and 15 show image results obtained for two values of s ($s \to \infty, s = 0.5$) and $\alpha = 0.1$ and $k = -1$. We can see that the best detection is obtained when s represents the real value.

Fig. 10. Image with additive Gaussian noise ($\sigma = 50$).

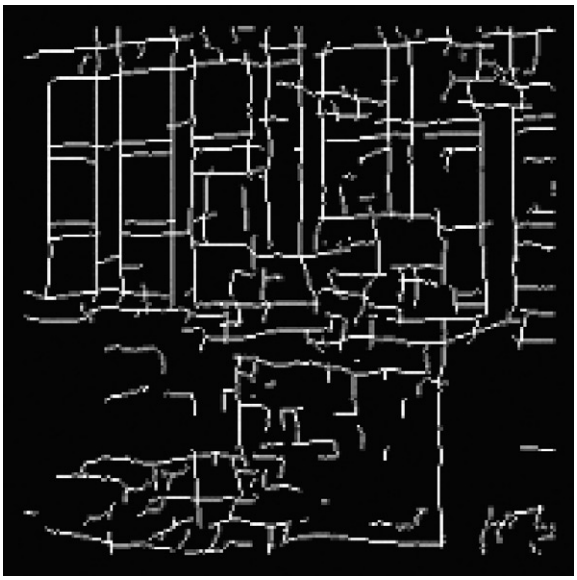

Fig. 12. Edges detected using optimal filter with $\alpha = 0.8$ and $s = 0.5$.

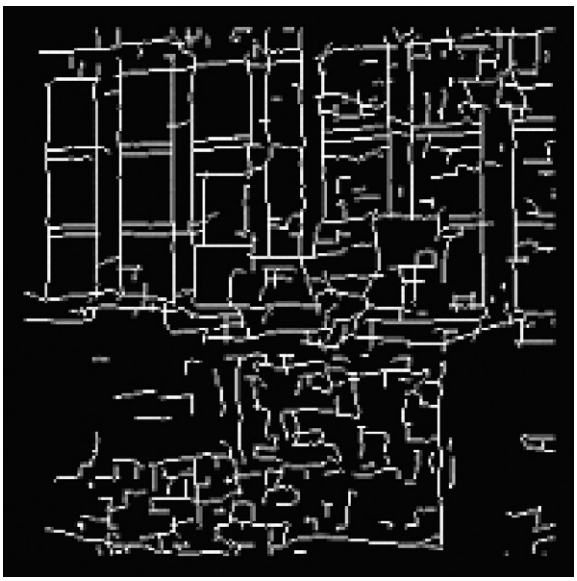

Fig. 11. Edges detected using optimal filter with $\alpha = 0.8$ and $s = \infty$.

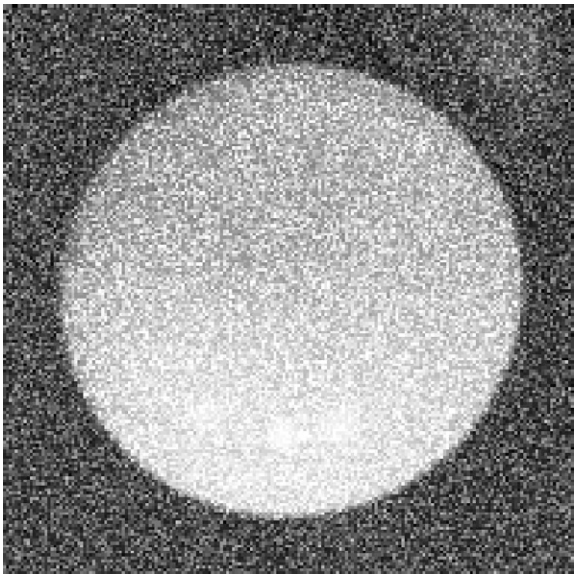

Fig. 13. Ball picture with additive Gaussian noise ($\sigma = 50$).

We also present in Table 1 some experimental values of implemented coefficients a_i according to the choice of the s and α parameters used for the extraction of contours.

9. Conclusion

In this paper we have presented an optimal operator for the detection of exponential shape edges. This

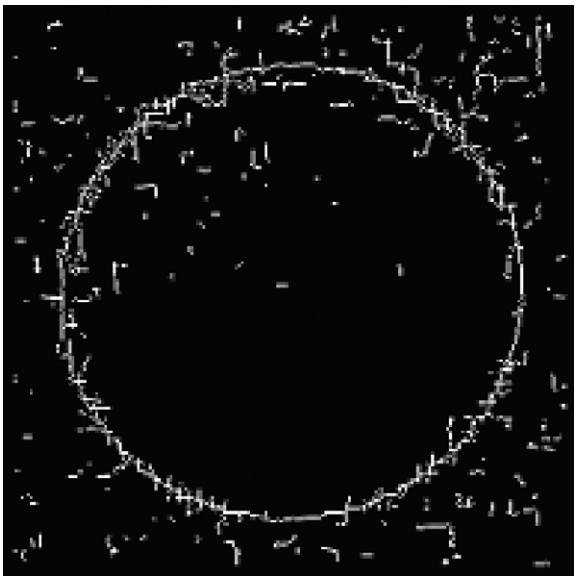

Fig. 14. Edges detected using optimal filter with $\alpha=0.8$ and $s=\infty$.

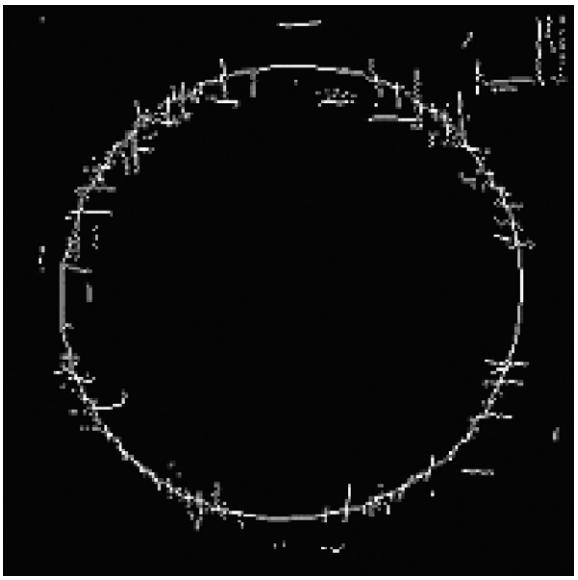

Fig. 15. Edges detected using optimal filter with $\alpha=0.8$ and $s=0.5$.

Table 1
Experimental values for implementing f filter (mathematical expressions of these coefficients are presented in Appendix B)

α	k	s	G	a_1	a_2	a_3	a_4	a_5
0.1	− 1	0.5	0.0018	− 7.7743	6.7646	− 2.4162	1.9164	− 0.4966
0.1	− 1	10	0.0050	− 0.9050	0.0002	− 1.8097	0.8188	− 0.0000
0.5	− 1	0.5	0.1276	− 0.6065	0.3679	− 1.8196	1.1036	− 0.2231
0.5	− 1	10	0.1236	− 0.6573	0.0308	− 1.2131	0.3679	− 0.0000
0.8	− 1	0.5	-1.74×10^{-4}	0.621×10^{3}	-0.279×10^{3}	− 1.5052	0.7470	− 0.1225
0.8	− 1	10	0.2587	− 0.6978	0.1117	− 0.8987	0.2019	− 0.0000

exponential function is an approximation model of real edges in most images obtained with CCD cameras.

With this aim, we followed the way paved by Canny and have therefore calculated three criteria: localization, signal-to-noise ratio, and multiple responses. The optimization of these criteria led us to a third-order recursive filter. The performances of this filter are determined for a given s, the best choice of the two parameters α (α determines the width of the filter) and k. These performances show an increase of the product of the signal-to-noise ratio by the localization of about 32% in the case of blurred and noisy images in comparison with a filter designed with an ideal edge model (model proposed by Canny and developed by Deriche).

The function filter we present in this paper (third-order filter) is a global filter. So it contains Deriche's second-order filter and Shen's first-order filter.

We have also found that for a given scene characterized by a parameter s, we can improve the edge detection with an optimal choice of the parameter α and k. So in the case of noisy and blurred images, the optimized filter allows us to increase the best signal-to-noise ratio and also the best localization of the edges. These performances are theoretically estimated by Cane's criteria and experimentally measured.

The recursive implementation of this filter allows us to avoid truncating the filter impulse response. This leads to an easy use of the optimized filter for multi-scale applications [1,2,7].

Appendix A. Resolution of Euler's equation

$$Z_f - \frac{d(Z_{f'})}{dx} + \frac{d^2(Z_{f''})}{dx^2} = 0$$

with

$$Z_f = \frac{dZ}{df} = 2f(x) + \lambda_3 e^{sx} + \lambda_4(1 - e^{sx}),$$

$$Z_{f'} = \frac{dZ}{df'} = 2\lambda_1 f'(x) \Rightarrow -\frac{d(Z_{f'})}{dx} = -2\lambda_1 f'' Z_{f''}$$

$$= 2\lambda_2 f''(x) \Rightarrow \frac{d^2(Z_{f''})}{dx^2} = 2\lambda_2 f''''.$$

When we change these values in Euler's equation, we obtain

$$2f - 2\lambda_1 f'' + 2\lambda_2 f'''' = (\lambda_4 - \lambda_3)e^{sx} - \lambda_4.$$

The solution of this differential equation is obtained in two steps:

A.1. Solution without second member

$$2f - 2\lambda_1 f'' + 2\lambda_2 f'''' = 0.$$

The general equation without second member admits as solution an exponential function

$$f(x) = be^{\xi x}.$$

We substitute this solution in the differential equation above; which leads to the characteristic equation hereafter:

$$1 - \lambda_1 \xi^2 + \lambda_2 \xi^4 = 0.$$

The resolution of this equation leads to the final solution hereafter

$$\xi^2 = \frac{\lambda_1}{2\lambda_2} \pm \frac{\sqrt{\lambda_1^2 - 4\lambda_2}}{2\lambda_2}.$$

We define

$$\xi = \pm\alpha \pm i\omega.$$

Which leads to two equations

$$\alpha^2 - \omega^2 = \frac{\lambda_1}{2\lambda_2}$$

$$4\alpha^2\omega^2 = \frac{\lambda_1^2 - 4\lambda_2}{4\lambda_2^2}.$$

From this last relationship, we deduce λ_1 and λ_2 which depend on α and ω

$$\lambda_1 = \frac{2(\alpha^2 - \omega^2)}{4\alpha^2\omega^2 + 4(\alpha^2 - \omega^2)^2},$$

$$\lambda_2 = \frac{1}{4\alpha^2\omega^2 + 4(\alpha^2 - \omega^2)^2}.$$

As $\omega \ll 1$

$$\lambda_1 \approx \frac{1}{2\alpha^2},$$

$$\lambda_2 \approx \frac{1}{4\alpha^4}.$$

The general solution of the differential equation without the second member is similar to that obtained by Canny [3].

$$f_0(x) = a_1 e^{\alpha x}\sin\omega x + a_2 e^{\alpha x}\cos\omega\xi + a_3 e^{-\alpha x}\sin\omega x + a_4 e^{-\alpha x}\cos\omega x.$$

A.2. General solution

The particular solution is

$$f_p(x) = \frac{(\lambda_4 - \lambda_3)e^{sx}}{2[1 + s^2(s^2\lambda_2 - \lambda_1)]} - \frac{\lambda_4}{2}.$$

The general solution is

$$f(x) = f_0(x) + f_p(x).$$

When one applies the limit conditions quoted in part 2:

$$f(-\infty) = 0 \Rightarrow a_3 = a_4 = \lambda_4 = 0,$$

so

$$f(x) = a_1 e^{\alpha x}\sin\omega x + a_2 e^{\alpha x}\cos\omega x - \frac{\lambda_3 e^{sx}}{2[1 + s^2(s^2\lambda_2 - \lambda_1)]}, \quad x \leqslant 0,$$

$$f(0) = 0 \Rightarrow a_2 = \frac{\lambda_3}{2[1 + s^2(s^2\lambda_2 - \lambda_1)]}.$$

Then

$$f(x) = a_1 e^{\alpha x}\sin\omega x + a_2 e^{\alpha x}\cos\omega x - a_2 e^{sx}, \quad x < 0.$$

Appendix B. Coefficients of the recursive implementation of the derivative filter

Numerical expression of the filter function

$$f(n) = (n + A)e^{\alpha n} - Ae^{sn}, \quad n \leqslant 0.$$

With

$$A = \frac{4}{3}\frac{k\alpha^4}{\omega(4\alpha^4 + s^4 - 2s^2\alpha^2)}.$$

Z transformation of $f(n)$

$$TZ^+ = \frac{a_1 z^{-1} + a_2 z^{-2}}{1 - a_3 z^{-1} + a_4 z^{-2} - a_5 z^{-3}} = \frac{Y^+(z)}{X(z)},$$

$$TZ^- = -\frac{a_1 z + a_2 z^2}{1 - a_3 z + a_4 z^2 - a_5 z^3} = \frac{Y^-(z)}{X(z)}.$$

Expression of the constants a_i

$$a_1 = \frac{A}{e^\alpha} - \frac{A}{e^s} - \frac{1}{e^\alpha}$$

$$a_2 = \frac{A}{e^\alpha e^s} + \frac{1}{e^\alpha e^s} - \frac{A}{(e^\alpha)^2},$$

$$a_3 = -\frac{2}{e^\alpha} - \frac{1}{e^s},$$

$$a_4 = \frac{1}{(e^\alpha)^2} + \frac{2}{e^\alpha e^s}$$

$$a_5 = \frac{1}{(e^\alpha)^2 e^s}$$

The constant of normalization G

$$\frac{1}{G} = -\left(2\frac{-Ae^{2\alpha} - e^{(\alpha+s)} + e^\alpha + Ae^\alpha + Ae^{(\alpha+s)} - Ae^s}{(2e^\alpha - 1 - e^{(2\alpha)})(e^s - 1)}\right).$$

References

[1] E. Bourennane, Conception et implantation d'un détecteur de contours optimisé sous forme d'un circuit ASIC, Université de Bourgogne, Thése de doctorat, Dijon, 1994.

[2] E. Bourennane, M. Paindavoine, F. Truchetet, Amélioration du filtre de Canny Deriche pour la détection des contours sous forme de rampe, Traitement du Signal 10 (4) (1993) 297–310.

[3] J. Canny, A computational approach to edge detection, IEEE Trans. Pattern Anal. Mach. Intell. PAMI-8 6 (November 1986) 679–714.

[4] R. Courant, D. Hilbert, Methods of Mathematical Physics, Vol. 1, Wiley-Intersciences, New York, 1953.

[5] R. Deriche, Using Canny's criteria to derive a recursively implemented optimal edge detector, Internat. J. Vision, Boston, 1987, pp. 167–187.

[6] R. Deriche, Fast algorithms for low—level vision, Ninth ICPR, Rome, November 1988, pp. 434–438.

[7] O. Laligant, F. Truchetet, E. Bourenanne, Multiscale edge detection with frames of optimized wavelets, International Conference on Wavelets, Messina, Italy, October 1993.

[8] W.H.H.J. Lunscher, The asymptotic optimal frequency domain filter for edge detection, IEEE Trans. Pattern Anal. Mach. Intell. PAMI-5 6 (November 1983) 678–679.

[9] D. Marr, E. Hildreth, Theory of edge detection, Proc. Roy. Soc. London 207 (1980) 187–217.

[10] J.W. Modestino, R.W. Fries, Edge detection in noisy images using recursive digital filter, Comput. Graphics Image Process. PAMI-1 6 (1977) 409–433.

[11] M. Petrou, J. Kittler, Optimal edge detectors for ramp edges, IEEE Trans. Pattern Anal. Mach. Intell. 13 (5) (May 1991) 1483–1491.

[12] S.O. Rice, Mathematical analysis of random noise, Bell Syst. Tech. J. 24 (1945) 46–156.

[13] L. Roberts, Machine perception of three dimensional solids. In J.T. Tippet and coworkers (Ed.), Optical and Electro-optical Information Processing, 1965, 159–197, MIT Press, Cambridge, Mass.

[14] S. Sarkar, K. Boyer, On optimal infinite impulse response edge detection filters, IEEE Trans. Pattern Anal. Mach. Intell. 13 (11) (November 1991) 1154–1171.

[15] K.S. Shanmugam, J.A. Green, An optimal frequency domain filter for edge detection in digital pictures, IEEE Trans. Pattern Anal. Mach. Intell. 1 (January 1979) 37–49.

[16] J. Shen, C. Castan, An optimal linear operator for edge detection, Proceeding Conference on Vision and Pattern Recognition (CUPR), Miami (1986) 109–114.

[17] L.A. Spacek, Edge detection and motion detection, Image Vision Comput. 4 (1986) 43–56.

[18] H.D. Tagare, R.J.P. de Figueiredo, On the localization performance measure and optimal edge detection, IEEE Trans. Pattern Anal. Mach. Intell. 12 (12) (December 1990) 1186–1190.

[19] V. Torre, T. Poggio, On edge detection, IEEE Trans. Pattern Anal. Mach. Intell. PAMI-8 2 (March 1986) 147–163.

[20] F. Truchetet, O. Laligant, E. Bourenanne, Frame of wavelets for edge detection, International Symposium on Optics, Imaging and Instrumentation, SPIE Proceedings, Vol. 2303, San Diego, July 1994, pp. 141–152.